# Generation of Broadband Electrostatic Waves in Earth's Magnetotail

Crockett Grabbe

*Department of Physics and Astronomy, University of Iowa, Iowa City, Iowa 52242*
(Received 28 April 1999)

The theory that broad-band electrostatic waves (BEN) in Earth's magnetotail are trapped-electron ("BGK") modes is reexamined. Electron/ion beams analyzed for a realistic magnetized-plasma source model with $\kappa$ distributions are found to drive an unstable spectrum of broad angular range over several orders of magnitude in $f$, up to $(0.1-0.2)f_{pe}$. Analysis indicates that trapping essential for the BGK paradigm is good only at the highest $f$, whereas most of the spectrum has minimal trapping and can be driven by electron/ion beam instabilities. A new model is proposed in which trapped-electron modes exist only at the highest $f$ band, whereas electron/ion beam instabilities drive the bulk of the broad-band spectrum below that. BEN wave data from ISEE-1 and ISEE-3 show large angles of propagation with respect to the magnetic field for $f < f_{ce}$ as predicted by the new model but not the BGK model. However $f > f_{ce}$ is observed only in a narrow angular range around the magnetic field and may be BGK modes. This predicts that the BEN solitary waves in the source region are not in BEN well into the lobe.

*1. Introduction.*—The origin of intense broad-band electrostatic waves (BEN) in the plasma sheet boundary layer (PSBL) of the magnetotail has been actively investigated since their discovery [1]. A model involving the ion acoustic instability driven by ion beams was proposed for its origin concurrent with a study of particle and wave data that showed a correlation of the waves with the high-energy streaming ions [2]. Subsequent theoretical analysis of these ion beam modes predicted that the beams can also drive an ion two-stream instability necessary for lower frequencies ($f$) and an instability associated with cold electrons that is essential for the high-$f$ part of the spectrum [3]. No data supporting the existence of these cold electrons have been published.

A new model was proposed in conjunction with the discovery in geotail data obtained by the Wave Form Capture receiver of spiky pulses a few milliseconds in length in BEN [4]. A simulation model was proposed [5] in which BEN are interpreted as trapped-particle (BGK) modes which develop from electron beam-instability saturation due to nonlinear trapping [6]. In a follow-up set of simulations different configurations involving counterstreaming electron beams and an ion beam were further examined for a magnetic-field-free plasma [7]. These were presented as models for BEN and narrow-band electrostatic noise (the latter was modeled as an electron-hole mode in the theory presented by [8]). A theoretical analysis was made of the BGK modes in [9], which were similarly modeled as bunches of electrons trapped by the wave potential pulse in a magnetic-field-free plasma.

Both simulation studies as well as the analytical study used idealistic assumptions by neglecting the background magnetic field and the ion dynamics. These call the validity of this model into question for the bulk of the observed BEN spectrum for several reasons. (1) The observed $f$ of the broad-band waves ranges from substantially below the electron cyclotron frequency $f_{ce}$ (electrons strongly magnetized) up to well over $f_{ce}$ (electrons weakly magnetized). The unmagnetized assumption used in the BGK model is definitely invalid for electrons (crucial for the trapping) unless $f \gg f_{ce}$ and other restrictions are satisfied (see, e.g., [10]). The first condition is satisfied only at the very top of the broad-band spectrum ($f \sim f_{pe}$, the plasma frequency). Since typically $f_{ce} \sim 0.1 f_{pe}$ in the BEN source regions, the conditions are incorrect for most of the frequency range of the broad-band spectrum, which extends down to just below $f_{lh}$, the lower hybrid frequency for hydrogen. The unmagnetized assumption is not valid for the bulk of the broad-band wave spectrum. (2) The magnetic field terms which were ignored in the analysis significantly alter the trapping process in BGK waves, as shown by data and theory discussed in Sec. 3. (3) The importance of standard instabilities of electron beams, the assumed energy source in the BGK model, has received little investigation and must also be examined before certain questions on the origin of BEN can be answered.

Models for BEN are reexamined with the magnetic field and ion dynamics included, and realistic $\kappa$ distributions are used. Problems with the trapped-electron (BGK) model are exposed, and an alternative model is proposed. In Sec. 2 a case of standard instabilities driven by electron and ion beams for a realistic plasma model for the midtail PSBL with observed $\kappa$ distributions is examined and is found to produce a substantial growth rate up to about 10%–20% of $f_{pe}$ and out to angles that are quite oblique to the magnetic field. These can strongly affect the trapping essential for the BGK models that have dominated the theory since the geotail discovery. Important questions on trapping and an alternative model are examined in Sec. 3.

*2. Linear and nonlinear instabilities.*—The importance of standard processes from electron and ion flow (the energy sources) through the magnetized plasmas with realistic $\kappa$ distributions and ion dynamics needs investigation for broad-band wave generation. The generation

region ranges over many Earth radii in the plasma sheet; at any given time and position it may vary from a primarily linear process to a primarily nonlinear process according to the variation in local conditions. Standard instabilities driven by the same energy sources as those used in the BGK model studies must be scrutinized for their possible role in the evolution of the spectrum. This is necessary for developing realistic models for the source of BEN before acceptance of highly idealized nonlinear models.

Kappa distributions are appropriate for modeling this magnetotail region; measurements of the particle distributions there indicate $\kappa \simeq 6-7$ for both electrons and ions (the limit $\kappa \to \infty$ corresponds to a Maxwellian) [11]. We recently analyzed and developed a new numerical method for rapidly and accurately evaluating the modified plasma dispersion function (MPDF, which for $\kappa \to \infty$ reduces to the well-known PDF) that occurs in the dispersion analysis for hot plasmas with generalized $\kappa$ distributions, for $|\kappa| > 3$ [12]. The numerical routines for calculating the MPDFs were used in the development of a vectorized kinetic code on the Cray-98/8128 at the San Diego Supercomputer Center for solving the growth rate and spectrum of instabilities in plasmas with $\kappa$ particle distributions and arbitrary parameters over a range of wave number $k$ and axial angular range $\theta$ with respect to the magnetic field.

The kinetic code was used to visually investigate electrostatic waves driven by electron beams (as assumed in the simulation models in [5,7]), with $\kappa = 7$ chosen for the electron and ion beams and background distributions, and $f_{ce}/f_{pe} = 0.1$, which is typical for the mid-distant tail. In Fig. 1 is a 3D plot of the spectrum produced for the case of a model with both electron and ion beams, as well as electron and ion backgrounds, with parameters chosen in the typical range of midtail observations [2]. The height of the surface (color) is for $\ln(\gamma/2\pi f_{ci})$, where $\gamma$ is the growth rate and $f_{ci}$ is the ion cyclotron frequency (for hydrogen ions). The base axes of the surface are $\ln(f\cos\theta/f_{ci})$ and $\ln(f\sin\theta/f_{ci})$ (numbers on the axes are orders of magnitude). The three-dimensional graph shows that instabilities can be driven up to 83° with respect to the magnetic field for $f$ up to $(0.1-0.2)f_{pe}$.

Much effort went into developing a code sensitive to $\kappa$, and the results for this case are noticeably sensitive to its value. At small angles for $\kappa = 7$ electrons in Fig. 1, the maximum growth $\gamma_m$ and upper frequency cutoff $f_c$ of the positive growth area can be $(2-3)\times$ smaller than it is for Maxwellian electrons. However, for larger angles $\gamma_m$ and $f_c$ can be $(3-4)\times$ larger for $\kappa = 7$ electrons than for Maxwellian electrons.

The results in Fig. 1 are fairly robust for the condition $f_{ce} \ll f_{pe}$. Earlier studies on ion beam instabilities showed waves could be driven up to the order of $f_{ce}$ and to quasiperpendicular angles of propagation, with growth rates approaching that of $f$. The results here are qualitatively similar for the range typical of the midtail region. A model for BEN *must* include the magnetic field for the lower bulk of frequencies at which these instabilities at
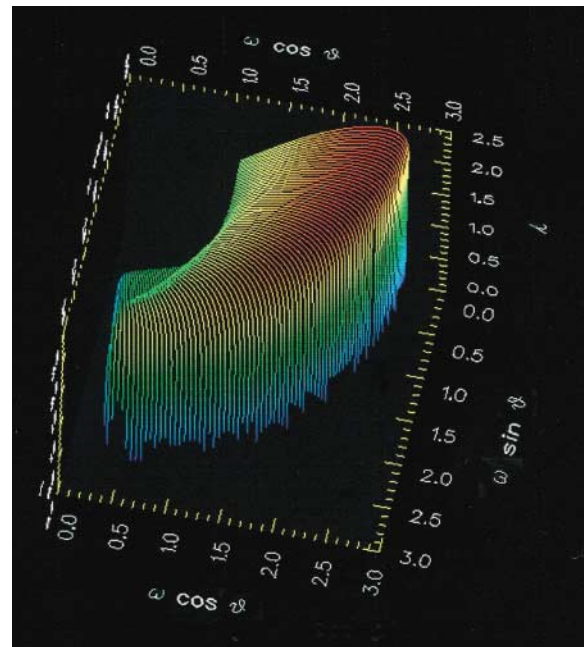


FIG. 1 (color). Three-dimensional spectrum of instabilities driven by energetic electron and ion beams and background distributions for $\kappa = 7$ and $\omega_{pe}/\omega_{ce} = 0.1$. The electron beam (with 40% of the total electron density) and ion beam (with 40% of the ion density) have a kinetic energy ratio of 0.2. The electron and ion beam temperatures are 10% of their kinetic energy. Instabilities driven by the electron and ion beams occur for $\theta$ (the angle with respect to the background magnetic field) up to 84° and frequency $f$ up to 20% of $f_{pe}$. The horizontal axis labeled $\omega\sin\theta$ corresponds to $\ln[(2\pi f/f_{ci})\sin\theta]$ and the axis labeled $\omega\cos\theta$ corresponds to $\ln[(f/f_{ci})\cos\theta]$, where $\theta$ is the angle of **k** with respect to the magnetic field. The vertical axis (labeled $\gamma$) corresponds to $\ln(\gamma/2\pi f_{ci})$. The surface is enhanced by colors, with red showing the greatest $\gamma$, followed by yellow, green, then blue.

large oblique angles can occur, because they play an essential role in the nonlinear trapping of electrons.

Over most of the unstable spectrum in Fig. 1 the growth rate $\gamma$ is as large as $2\pi f$. This is in striking contrast to the simulation of cases such as the warm bistream instability in [7]. Omura *et al.* indicate that the electron-hole mode is the one excited in their simulations for that case, and then they analyzed that mode through linear analysis for a Maxwellian distribution under the criterion that $\gamma \ll 2\pi f$. The gentle-bump instability, which has been identified as the linear instability that develops into BGK waves in the BGK model, has a similarly small $\gamma$. But the more realistic calculations of Fig. 1 show that the beams can drive instabilities with much larger $\gamma$ in BEN. Similar to previous models of ion beam instabilities [2,3], the instabilities for most of Fig. 1 show growth rates that are much too large to satisfy this criterion.

*3. Alternative model for the BEN spectrum.*—The streaming electrons and ions are the major energy source in this region of the magnetotail and undoubtedly fuel BEN. It was recognized from earlier studies that there are several instabilities ion beams can produce and that

likely multiple sources of these instabilities accounted for the BEN observations. The ion-beam model previously explored had the ion acoustic, two-stream, and Buneman instabilities as each producing parts of the spectrum [3]. The BGK models proposed in [4,5] are nonlinear extensions of the single electron bump-on-tail instability. Both models by themselves appear inadequate to account for BEN observations.

Figure 1 shows that large growth driven by both electron and ion beams can occur for $f$ up to about $(0.1-0.2)f_{pe}$. However, BEN is observed up to $f_{pe}$, so these standard instabilities appear not to drive the top of the frequency range observed. The condition for validity of neglecting nonlinear trapping in the wave analysis (i.e., for the wave approaching quasilinear saturation before any significant trapping can occur) is then that the "linear" time $t_L \ll t_{\text{tr}}$, the trapping time, or for the wave electric field $E$ [6]:

$$|\omega| \sim \gamma \gg (ekE/m_e)^{1/2} \qquad (1)$$

($\gamma$ is the growth rate and $\omega = 2\pi f + i\gamma$ is the complex frequency) since $\gamma \gtrsim 2\pi f$ for most of the unstable spectrum of the linear BEN waves driven by the beam instabilities (Fig. 1). For most of the unstable waves in this spectrum, $k$ is approximately $2\pi f/v_b$, with $v_b$ the electron beam velocity. Criterion (1) will be examined in wave data for BEN.

BEN source region observations at both magnetotail distances of $(10-20)R_E$ from ISEE-1 [2] and in the distant magnetotail ($R \sim 100R_E$) from ISEE-3 [13] put the observed upper limit of $E$ at about $5 \times 10^{-3}$ V/m for the upper $f$ of the unstable spectrum, which occurs typically at a few hundred kHz (near $0.1f_{pe}$). In Fig. 1, which exhibits optimal $\gamma$ at $f \sim 0.1f_{pe}$, one has $\gamma \sim 500$ s$^{-1}$, whereas $(ekE/me)^{1/2} < 10$ s$^{-1}$. Thus this criterion appears well satisfied in the BEN wave data for the unstable spectrum examined in Fig. 1, so standard beam instabilities are expected to persist and quasilinearly saturate before significant trapping can occur.

Not only does the unstable spectrum in Fig. 1 grow to a large amplitude before much electron trapping occurs, but electron cyclotron effects cannot be ignored as they have been in previous analyses for the BKG model [4,5,7,9]. Since the instabilities have a large angular range of electric field $\mathbf{E}$ direction, whereas the cyclotron effects tend to align electron beams along the magnetic field, perpendicular components of any stronger trapping forces will produce stronger $\mathbf{E} \times \mathbf{B}$ drifts away from such regions to regions of weaker $\mathbf{E}$, where that drift is much smaller and trapping much less significant. Thus particle motion oblique to the field counters any trapping that occurs in the non-field-aligned waves and decreases the ability for trapped-electron modes to form. Trapping is significant only when both the electron beams *and* the waves are approximately confined along the magnetic field to one dimension (analogous to trapping for shear Alfvén waves [14]). The conclusion is that all of the BEN spec-

trum except the highest-$f$ band is produced by these instabilities. As beam conditions always change, a linear/quasilinear mixture of the spectrum will be observed.

The instabilities driven by the electron beams disappear for $f$ above $0.2f_{pe}$ in Fig. 1. However, BEN is observed up to $f \simeq f_{pe}$. The measurements on geotail definitely show the presence of solitary wave pulses with typical pulse time on the order of $1/f_{pe}$ [4,7], so the waves corresponding to $f$ near $f_{pe}$ are apparently nonlinear in character and occur where standard beam instabilities may not exist. Simulations of these solitary waves arising from the gentle-bump instability in a magnetized plasma showed they are quite sensitive to the strength of the magnetic field and may disappear when $f_{ce} > f_{pe}$, which is consistent with this model [15].

Thus the model of trapped-particle modes set forth in various forms [5,7,9], which requires $f \gg f_{ce}$ for validity, applies only to wave forms such as the pulses that correspond to a nonlinear frequency band near $f_{pe}$ and is only a viable model for high $f$ of the BEN spectrum that is stable in Fig. 1. This high-$f$ restriction may allow one to neglect the magnetic field in its analysis, as has been done in simulations used to account for the double layer forms observed on geotail [4]. As one decreases $f$ of the observed BEN spectrum much below $f_{pe}$, magnetic field effects rise in importance, decreasing the nonlinear trapped-particle essence of the waves, until frequencies are reached near $(0.1-0.2)f_{pe}$ at which the standard beam instabilities occur and totally dominate over any nonstandard trapped-particle modes that may exist.

This new model, in which the solitary waves have characteristic frequency that lies close to $f_{pe}$ where the magnetic field effects are negligible, whereas the bulk of the broad-band spectrum which occurs at frequencies below that arises from beam instabilities where trapping is negligible, is further supported by the data on ISEE-1 crossing of the PSBL [2,16]. If the high-$f$ waves near $f_{pe}$ have a very different source process than the broad-band spectrum at lower frequencies, one should search for a noticeable demarcation that may exist in the wave spectrum that is observed. One does in fact see such a demarcation, and, furthermore, the data show that the lower-$f$ portion of BEN cannot involve significant trapping. Several examples of entry in the PSBL were discussed in the ISEE-1 data in [16]. Cases were shown of exit of the PSBL at 110 UT on day 048 of 1978; entry at 0225 UT on day 048, 0324 UT on day 060, 0357 UT on day 085, 1952 UT on day 154 (all of 1978); and entry at 0324 UT on day 084 of 1980. In all of those cases the lower frequency bulk (up to on the order of $f_{ce} \sim 700$ Hz) is observed well into the lobe up to before (on entry into) or after (on exit out of) crossing the PSBL. However, the high frequencies (up to on the order of the $f_{pe} \sim 5$ kHz) are first seen right near and after the time of spacecraft entry into, or last seen on exit from, the PSBL. In all cases the spacecraft was moving at a relatively large oblique angle with respect to the magnetic field, with the beams and lobe-PSBL transition
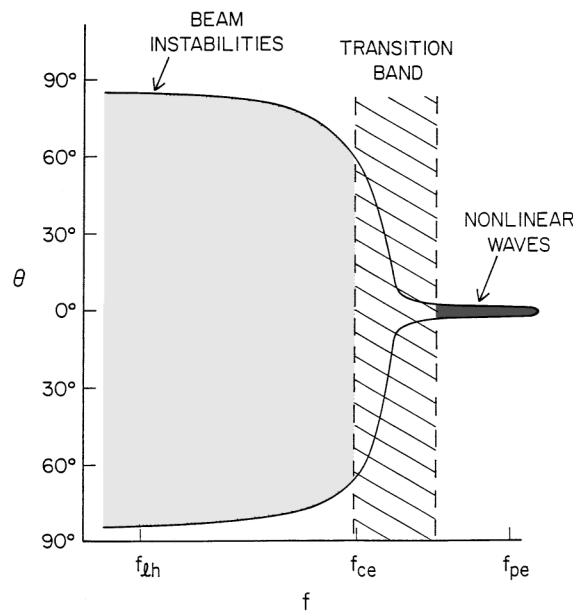
FIG. 2. Summary of the angular spectrum in the proposed model for the source region. For the lower-$f$ bulk a wide-angle spectrum of BEN is driven by beam instabilities. As $f$ goes above $f_{ce}$ the instability spectrum starts to disappear, and the electron trapping starts becoming more significant. For $f$ above about $(3-4)f_{ce}$, the magnetic field effects become negligible and nonlinear waves approximating BGK equilibria can exist. Note that for these waves the Fourier transform in $f$ is no longer valid, so the spectrum is not adequate for describing the structures of that observed on geotail.

closely aligned along the magnetic field. Thus the $f$ spectrum observed while the spacecraft was well into the lobe had substantial components of propagation perpendicular to the magnetic field lines. This is in contrast to the behavior of trapped-particle modes, which would be highly field aligned since they would travel in the direction of the electron beam which is highly field aligned. However, the wave spectrum is quite consistent with the electron/ion beam instability spectrum in Fig. 1. On the other hand the very high $f$ band, which is clearly quite field aligned because of its sudden appearance near the crossing time, would be consistent with the behavior of trapped-particle modes. Thus the observations support this new model, which is summarized in the graph of Fig. 2.

An interesting prediction arises from this new model since the nonlinear trapping structures are confined to the highest frequencies and are roughly field aligned, whereas beam instabilities produce the bulk of the waves at frequencies below that, which are spread at wide angles with respect to the magnetic field. The PSBL (the source region) runs along the magnetic field, so if the hooks (solitary wave structures) observed on geotail are trapping structures, they would be confined to the area near the PSBL. However, the instability spectrum, which is in a large angular range where trapping is minimal, will spread well out into the lobe. Thus as the spacecraft crosses the lobe approach-

ing the PSBL, this model predicts that it should observe a spatial evolution of the spectrum from a broad-band one with an upper $f$ limit well below $f_{pe}$ into one with strong solitary waves present in the temporal wave forms as the spacecraft enters the PSBL. These solitary waves should not be present well away from the PSBL. These predictions will be a topic of future investigation.

[1] D. A. Gurnett, L. A. Frank, and D. Lepping, J. Geophys. Res. **83**, 5217 (1978).

[2] C. L. Grabbe and T. E. Eastman, J. Geophys. Res. **89**, 3865 (1984); **89**, 3977 (1984).

[3] C. L. Grabbe, Geophys. Res. Lett. **12**, 483 (1985); in *Advances in Space Plasma Physics,* edited by B. Buti (World Scientific, Singapore, 1985), pp. 356–381; N. Omidi, J. Geophys. Res. **90**, 12 330 (1985).

[4] H. Kojima, H. Matsumoto, T. Miyatake, I. Nagano, A. Fujita, L. A. Frank, T. Mukai, W. R. Paterson, Y. Sato, S. Machida, and R. R. Anderson, Geophys. Res. Lett. **21**, 2919 (1994); H. Matsumoto, H. Kojima, T. Miyatake, Y. Omura, M. Okada, I. Nagano, and M. Tsutsui, Geophys. Res. Lett. **21**, 2915 (1994).

[5] Y. Omura, H. Kojima, and H. Matsumoto, Geophys. Res. Lett. **21**, 2923 (1994).

[6] I. Bernstein *et al.,* Phys. Rev. **108**, 546 (1957) [reprinted in C. L. Grabbe, *Plasma Waves and Instabilities* (American Association of Physics Teachers, College Park, MD, 1986)]; R. C. Davidson, *Methods in Nonlinear Plasma Theory* (Academic Press, New York, 1972); H. Schamel, Phys. Rep. **140**, 161–191 (1986).

[7] Y. Omura, H. Matsumoto, T. Miyake, and H. Kojima, J. Geophys. Res. **101**, 2685 (1996).

[8] F. V. Coriniti and M. Ashour-Abdalla, Geophys. Res. Lett. **16**, 747–750 (1989); F. V. Coriniti, M. Ashour-Abdalla, and R. L. Richard, J. Geophys. Res. **98**, 11 349–11 358 (1993).

[9] V. I. Krasovsky, H. Matsumoto, and Y. Omura, J. Geophys. Res. **102**, 22 131 (1997).

[10] P. A. Robinson, Phys. Fluids **31**, 525 (1988).

[11] S. P. Christon, D. G. Mitchell, D. J. Williams, L. A. Frank, C. Y. Huang, and T. E. Eastman, J. Geophys. Res. **93**, 2562–2572 (1988).

[12] C. L. Grabbe and E. Venturino, Phys. Plasmas **3**, 35 (1996); D. Summers and R. M. Thorne, Phys. Fluids B **3**, 1835 (1991).

[13] F. V. Coriniti, E. W. Greenstadt, B. T. Tsuritani, E. J. Smith, R. D. Zwickel, and J. T. Gosling, J. Geophys. Res. **95**, 20 977 (1990).

[14] M. V. Medvedev, P. H. Diamond, M. N. Rosenbluth, and V. I. Schevchenko, Phys. Rev. Lett. **81**, 5824 (1998).

[15] T. Miyake, Y. Omura, H. Matsumoto, and H. Kojima, J. Geophys. Res. **103**, 11 841 (1998).

[16] C. L. Grabbe, J. Geophys. Res. **94**, 17 299 (1989); **94**, 17 329 (1989).